ELSEVIER

Journal of Alloys and Compounds 293–295 (1999) 14–18

Journal of ALLOYS AND COMPOUNDS

High-pressure studies of Laves phase intermetallic hydrides – Adaptation of statistical thermodynamic models

O. Beeri[a,b,*], D. Cohen[a], Z. Gavra[a,b], J.R. Johnson[c], M.H. Mintz[a,b]

[a]*Nuclear Research Center-Negev, P.O. Box 9001, Beer-Sheva, Israel*
[b]*Ben-Gurion University of the Negev, P.O. Box 653, Beer-Sheva, Israel*
[c]*Brookhaven National Laboratory, P.O. Box 5000, Upton, NY 11973-5000, USA*

Abstract

Pressure–composition isotherms of unstable intermetallic hydrides of some Laves phases ($TiCr_{\sim 2}$, TiCrMn) were measured over a wide pressure range up to 1000 atm H_2. These measurements enabled the evaluation of the critical temperatures, T_c, of the respective systems as well as the derivation of their thermodynamic characteristics above T_c. For this one-phase high-temperature range, simplified statistical-thermodynamics models can be adapted to calculate analytical forms of the corresponding isotherms. A comparison between the model-derived and the experimental isotherms then yields the average pairwise nearest neighbor H–H interaction parameter, η, and its temperature dependence. In the present study, a rigid-metal sublattice model was utilized and solved employing the conventional Bragg–Williams (BW) and Quasi-Chemical (QC) approximations. In fact, both approximations resulted in similar $\eta(T)$ values, as well as close estimates of T_c. For the $TiCr_{\sim 2}$–H_2 system the above analysis indicated that η changes from attractive (i.e., negative) to repulsive (i.e., positive) with increasing isotherm temperatures. This trend was qualitatively interpreted as resulting from the net interplay of two energy terms, the elastic strain contribution, which induces an effective attractive interaction, and the electrostatic contribution which adds a repulsive term. For the TiCrMn–H_2 system, it turned out that the partial substitution of chromium by manganese had only a minor effect on the stability of the hydride, however, it pronouncedly increased the critical temperature (T_c) of the system. This observation can be accounted for by the simultaneous electronic and structural effects of manganese in this compound.

Keywords: High-pressure; Hydrides; $TiCr_{1.8}$; Thermodynamics; Statistical-thermodynamics

1. Introduction

There have been considerable experimental efforts during the last two decades in studying the thermodynamic and structural properties of intermetallic hydride systems [1–3]. Most of these studies were conducted on hydrides of intermediate stabilities (i.e., having plateau pressures in the range of 1–20 atm at ambient temperature), where pressure–composition (p–c) isotherms were evaluated mostly below the critical temperatures, T_c, of the investigated systems. Such experimental properties are in fact more relevant for most applications of intermetallic hydrides, and are also easier to investigate from an experimental point of view.

It has been pointed out recently [4] that obtaining p–c isotherms above T_c may provide novel fundamental information regarding microscopic, energy-related parameters, associated with the pairwise nearest neighbor H–H interactions controlling the phase transition behavior of these hydrides. Yet, for the intermediate-stability hydrides, the corresponding T_c values are too high to maintain the (metastable) intermetallic structure, and irreversible phase decomposition usually takes place within this temperature region. Conversely, for unstable hydrides, such as those of the $TiCr_{\sim 2}$ system [5–7], low T_c values are involved, which makes such supercritical measurements possible. Evidently, the corresponding p–c isotherms fall within a very high-pressure range (many hundreds of atmospheres), and special very-high pressure (VHP) equipment is required for such experiments.

This approach has recently been applied to study the supercritical isotherms of the $TiCr_{1.8}$–H_2 system [4]. The experimental isotherms were then compared to some analytical functions resulting from conventional statistical thermodynamics models [8–12], from which the pairwise nearest neighbor H–H interaction parameter, $\eta(T)$, and its temperature dependence were evaluated. These preliminary experiments [4] were in fact performed on $TiCr_{1.8}$ samples

*Corresponding author.

0925-8388/99/$ – see front matter
PII: S0925-8388(99)00382-5

which contained a mixture of cubic C15 and hexagonal C36 [4,13] allotropic forms of this compound. In the present study, we used more homogeneous samples which contained a nearly single-phase C15 structure. In addition, the effects induced by the partial substitution of chromium by manganese were compared using TiCrMn (C14 structure). The effects of structure related parameters and of electronic–electrostatic parameters on the pairwise interaction parameter $\eta(T)$ are then discussed.

2. Experimental

The details of the experimental procedures applied to alloy preparation, and in p–c isotherm determination as well as a description of the VHP Sieverts system (operating up to about 1000 atm), and the tedious set of calibration procedures and calculations required for an accurate determination of the H/M composition ratios (within an accuracy of ± 0.02) were presented in a previous publication [4].

In the present study two Laves phase intermetallics are compared. The first — $TiCr_{1.8}$, which contains nearly single phase cubic (C15) intermetallic [5,13], and the second — TiCrMn compound, which has the hexagonal (C14) structure [14]. It is worth mentioning that it is very difficult to prepare a nearly single phase cubic $TiCr_{1.8}$ C15 without the presence of the additional hexagonal C36 phase [5,13]. The present samples of the $TiCr_{1.8}$ compound contain about 90% of the C15 phase (as compared to the C15:C36 mixed phases of about 50:50% used in Ref. [4]).

3. The statistical model

The experimental p–c isotherms were fitted to the analytical expressions derived by a simplified statistical thermodynamics model [4,8–12]. The model assumes a ''rigid'' metal sublattice (i.e., maintaining its original structure at any H/M composition) with one type of tetrahedral interstitial sites which are occupied by H atoms (in our case the tetrahedral A2B2 sites are dominantly occupied [15]).

As discussed in Ref. [4], the assumption that the metal atoms sublattice is invariant with increasing hydrogen content, precludes the application of this model when the phase transition condition (i.e., $\alpha \rightarrow \beta$) is approached. Hence, the utilization of the model-derived p–c relation is justified only above the critical temperature of the system, T_c, when a single-phase solid solution of H in the parent metal is maintained throughout the whole composition range of the isotherm.

In solving the model, some approximations are assumed concerning the distributions of H atoms within the sublattice of interstitial sites. The most commonly used approximations are the zero order (BW) [8,9] and the first order (QC) [10–12] which yield isotherm expressions of the type [12]:

$$\ln\left[\frac{P_{H_2}(T)}{P^0_{H_2}(T)}\right] = F_j(\rho, z\cdot\eta, T) \tag{1}$$

with P_{H_2} — the equilibrium isotherm pressure; $P^0_{H_2}$ — the plateau (two-phase region) equilibrium pressure for temperatures below T_c, and the equilibrium pressure at $\rho = \frac{1}{2}$ (see below) above T_c; z — the number of nearest neighbor sites surrounding each H site in the interstitial sublattice; η — the pairwise interaction parameter between nearest neighbor H–H atoms ($\eta < 0$ for attractive interactions and $\eta > 0$ for repulsive ones); and ρ — the normalized H concentration, defined as:

$$\rho = \frac{N_H}{N_s} = \frac{(H/M) - (H/M)_{min}}{(H/M)_s - (H/M)_{min}} \tag{2}$$

with N_H — the number of H atoms in the lattice; N_s — the maximum available H sites; H/M — the atomic composition ratio; $(H/M)_s$ — the maximum H/M composition ratio obtained at infinitely high pressure; and $(H/M)_{min}$ — initial composition ratio where trapping of H precedes the ''normal'' occupation of interstitial sites [4].

The subscript j in Eq. (1) denotes either the BW or the QC approximations, with each yielding a somewhat different functional form of F_j [4].

Also, the critical temperature of the system can be derived by the condition:

$$\left.\frac{dF_j(T_c)}{d\rho}\right|_{\rho=1/2} = 0 \tag{3}$$

which yields for the two above approximations:

$$T_c^{BW} = -\frac{z\eta_{BW}}{4k} \tag{4}$$

$$T_c^{QC} = \frac{\eta_{QC}}{2k\ln\left[\frac{z-2}{z}\right]} \tag{5}$$

with k — the Boltzmann constant. (In Ref. [4], Eq. (5) was mistakenly written with a minus sign).

The pairwise interaction parameter, $\eta(T)$, can then be evaluated at any given temperature by fitting the experimental isotherm to the model-derived expressions (Eq. (1)).

For a temperature independent η, the calculated T_c value obtained by substituting η into Eq. (4) or Eq. (5) can then be compared with the observed one. However, if η changes with temperature, the explicit functional form of $\eta(T = T_c)$ should be substituted into Eq. (4) or Eq. (5) yielding a relation for T_c. By solving this relation the calculated value of T_c is then derived [4].

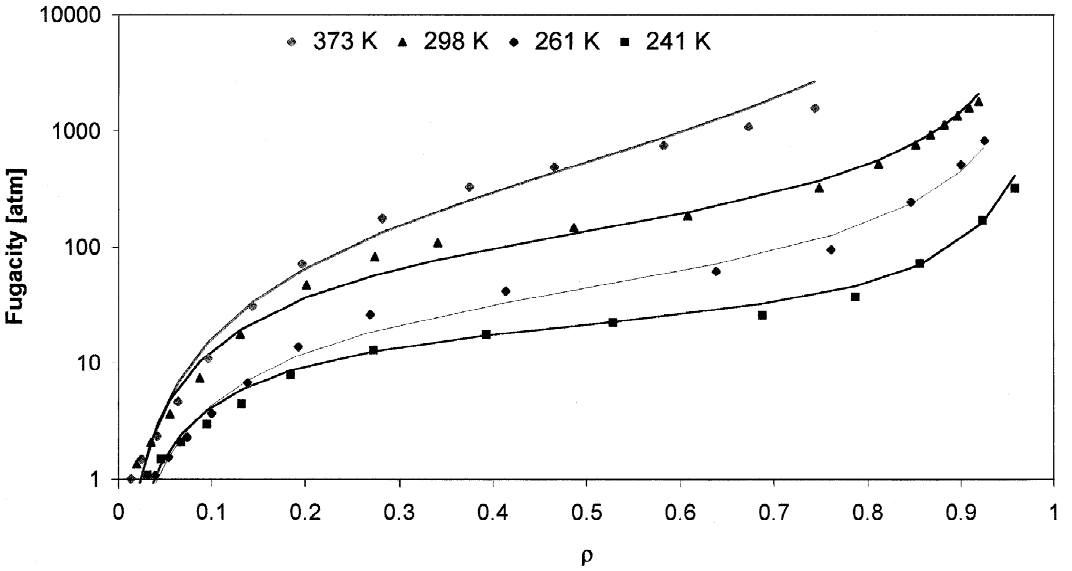

Fig. 1. The P–C desorption isotherms obtained for the $TiCr_{1.8}$ (C15 structure) — H_2 system at some selected temperatures. The solid lines represent the fit of the calculated expressions Eq. (1) (in this figure only the fit of the QC approximation is demonstrated), to the experimental data (points). The typical relative deviation of the fitted values from the observed ones is ~5% ($\ln(f_{observed}/f_{fitted})/\ln(f_{observed})$).

4. Results and discussion

Fig. 1 presents the P–C desorption isotherms obtained for the $TiCr_{1.8}$ (C15 structure) — H_2 system. The solid lines represent the fit of the calculated expressions Eq. (1) (in this figure only the fit of the QC approximation is demonstrated), to the experimental data (points). For this high-pressure range, all pressure units were corrected to fugacity values (f_{H_2}) according to the procedure outlined in Ref. [4]. Van't-Hoff plots of $\ln f_{H_2}$ vs. $1/T$, at a given H/M composition ratio, yields then the partial molal enthalpy, ΔH, and entropy, ΔS. Within this supercritical range (i.e., above T_c), a linear dependence of both thermodynamic quantities on H/M is obtained:

$$\Delta H(H/M) = a_H + b_H \cdot (H/M) \quad (6)$$

$$\Delta S(H/M) = a_S + b_S \cdot (H/M) \quad (7)$$

Table 1 summarizes $\Delta H + \Delta S$ desorption values as well as the a_H, b_H, a_S, b_S values obtained for the present samples as compared with the previously reported values obtained for $TiCr_{1.8}$ samples containing a mixture with much higher concentration of the C36 hexagonal phase [4,13]. It is seen that apparent differences are induced in these parameters by the C36 allotropic form, when present in the sample. However, as discussed below, the stability of these hydrides (given by ΔH ($\rho = 1/2$), ΔS ($\rho = 1/2$)) is not much affected by this additional phase, as proposed in Ref. [4].

Table 1
Thermodynamic values for the $TiCr_{1.8}$–H_2 system as a function of alloy purity

Parameter	$TiCr_{1.8}$ (present) (C15)	$TiCr_{1.8}$ ([4]) (C15+C36)
a_H [kJ/mole H_2]	13.0±0.4	8.8±1.7
b_H [kJ/mole H_2]	11.3±0.8	16.8±3.4
a_S [J/(K·mole H_2)]	71.47±2.09	30.90±2.47
b_S [J/(K·mole H_2)]	62.63±3.48	120.75±4.73
ΔH ($\rho = 1/2$) [kJ/mole H_2]	19.7±0.8	18.8±3.8
ΔS ($\rho = 1/2$) [J/(K·mole H_2)]	109.07±4.19	103.33±5.32

As pointed out previously [4] the conversion of the H/M composition ratio to ρ (normalized composition units, Eq. (2)) requires the estimation of the initial composition range corresponding to the ''trapping'' of hydrogen (i.e., $(H/M)_{min}$) in Eq. (2)), as well as the saturation, $(H/M)_S$, value. For the present $TiCr_{1.8}$ samples the parameters were similar to those reported before [4] (i.e., $(H/M)_{min} \approx 0.2$ $(H/M)_S \approx 1$). Utilizing Eqs. (2), (6) and (7) the thermodynamic molal enthalpy and entropy at $\rho = 1/2$ are derived, and compared to the previously reported ones [4] (Table 1), which indicate a similar thermodynamic stability for the two cases.

The fitted values of the pairwise H–H interaction parameter, $\eta(T)$, are plotted as a function of isotherm temperature in Fig. 2. As mentioned above, the solid lines in Fig. 1 represent the fitted model-derived isotherms (Eq. (1)) obtained by the QC approximation. However, fits were made for both, BW and QC approximations, and both fitted values of η are present in Fig. 2. It is seen that very similar results are obtained by both functions.

The temperature dependence of $\eta(T)$ is very interesting. At temperatures much higher than T_c the pairwise H–H interaction is repulsive (i.e., $\eta > 0$), however as the temperature is decreased this interaction converts into an attractive one ($\eta < 0$). Finally, as the temperature approaches T_c, the (attractive) interaction stabilizes on a

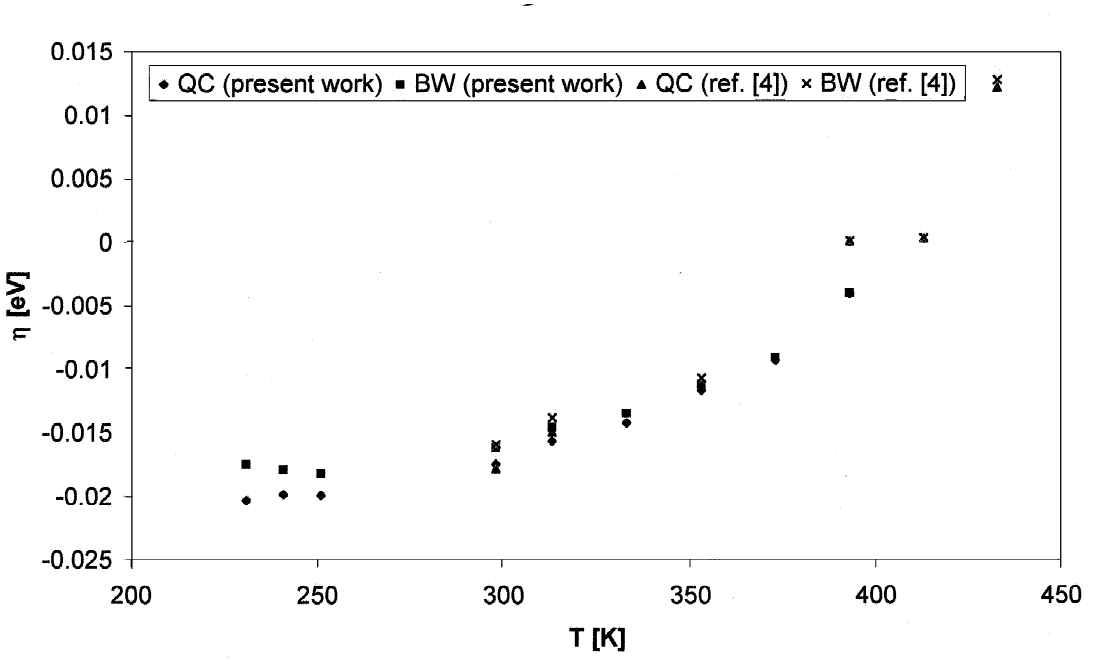

Fig. 2. The fitted values of the pairwise H–H interaction parameter, $\eta(T)$, as a function of isotherm temperature. A comparison is made with the values obtained in Ref. [4].

constant, temperature-independent value. The conversion of η from repulsive into attractive interaction occurring with decreasing temperature has been reported (for this system) in a recent publication [4]. However, the extension of the $\eta(T)$ vs. T plot to lower temperatures (down to T_c) has not been made there, and the leveling-off of this curve has not been pointed out (even though apparent in the presented data of Ref. [4] as demonstrated in Fig. 2). The temperature dependence of η was qualitatively accounted for [4] by the assumption of a combined contribution of an attractive, temperature-dependent elastic term and a repulsive, temperature independent electrostatic term (arising from the identical charging of adjacent sites with H atoms). As the temperature decreases, the contribution of the attractive term increases due to an increase in the elastic constants of the compound. This leads to the above mentioned changes in η. From the present results it turns out that if the above explanation holds, the temperature variation of the elastic constants becomes less pronounced as T approaches T_c, and finally levels off. Table 2 summarizes the limiting (constant) η values obtained by the two approximations, and the corresponding critical temperatures, calculated by substituting these η values into Eqs. (4) and (5) (from crystallographic consideration we chose $z=4$ for both, C15 and C14, structures [4,14–16]). It is seen that even though the fitted η parameters derived by the two approximations are similar, the calculated T_c values are higher for the BW approximation than for the QC one. This is easily verified by Eqs. (4) and (5) which indicate that for a given η value $T_c^{QC}/T_c^{BW}<1$ for $z>2$ (which is the case for a three-dimensional lattice). It should be noted that the present calculated T_c values (in Table 2) are significantly lower than those reported in Ref. [4]. This is due to the different calculation procedure applied in the previous study [4] where a linear temperature dependence of $\eta(T)$ was substituted into Eqs. (4) and (5). As mentioned above, the leveling-off of η on a constant, temperature-independent value (as T_c is approached) requires the substitution of this constant η into the T_c equations rather than a temperature-dependent $\eta(T)$ function. This leads to the above difference in the corresponding calculated T_c values.

A similar procedure applied to the hexagonal C14 structure of the TiCrMn [14] yields a temperature-invariant η which is more negative by about 130% than the corresponding limiting η value of the $TiCr_{1.8}$–H_2 system

Table 2
H–H interaction parameters and critical temperature values

Parameter	$TiCr_{1.8}$ (C15)		TiCrMn (C14)	
	QC	BW	QC	BW
η saturation [eV]	-1.99×10^{-2}	-1.78×10^{-2}	-4.27×10^{-2}	-3.59×10^{-2}
T_c calculated [K]	168	208	357	417

(see Table 2). Substituting this value into Eqs. (4) and (5) yields $T_c^{BW}=453$ K; $T_c^{QC}=377$ K which are higher then the $TiCr_{1.8}$ case. Experimentally, the measured T_c seems to correspond better to the QC value than to the BW evaluation. This illustrates the benefit of applying the higher order approximation when approaching the critical point.

Structure analysis of the C14 TiCrMn [16] as compared to the C15 $TiCr_{1.8}$ [16] indicates that for the tetrahedral A2B2 sites the interstitial volume size as well as the nearest neighbor distance between sites are smaller for the TiCrMn than for the $TiCr_{1.8}$. Both factors may lead to a more significant elastic term which induces an apparent more attractive pairwise interaction parameter. Yet, it is expected that the smaller volume size factor would also result in a more repulsive H-lattice interaction term which will lead to a less stable hydride. This expectation is not fulfilled, and the TiCrMn–H_2 system has in fact a stability (ΔH ($\rho=1/2$)$=19.76\pm0.16$ kJ/mole H_2, ΔS ($\rho=1/2$)$=106.60\pm0.59$ J/(K·mole H_2)) which is similar to that of the $TiCr_{1.8}$–H_2 (see Table 1). It is however possible that the increased elastic H-lattice interaction mentioned above is compensated by an opposite (i.e., stabilizing) term arising from a more attractive H–Mn electronic interaction. In that case, the overall stability of both compounds (i.e., TiCrMn and $TiCr_{\sim 2}$ hydrides) will be the same, with a more negative H–H pairwise interaction parameter apparent for the TiCrMn–H_2 system, due to the increased elastic term and the shorter H–H distance.

Acknowledgements

Thanks are due to Mr. A. Hemmy for his technical assistance. This research was supported by grant No. 9400094 from the United States–Israel Binational Science Foundation (BSF), Jerusalem, Israel.

References

[1] G. Sandrock, S. Suda, L. Schlapbach, in: L. Schlapbach (Ed.), Hydrogen in Intermetallic Compound II, Springer, Berlin, 1992, Chap. 5.
[2] E.L. Huston, G.D. Sandrock, J. Less-Common Met. 74 (1980) 435.
[3] M.A. Fetcenko, S.R. Ovshinsky, S. Veukatesan, K. Kojita, Third International Rechargeable Seminar, Deerfield Beach, FL, 1990.
[4] O. Beeri, D. Cohen, Z. Gavra, J.R. Johnson, M.H. Mintz, J. Alloys Comp. 267 (1998) 113.
[5] J.R. Johnson, J.J. Reilly, Inorg. Chem. 17 (1978) 3103.
[6] J.R. Johnson, J.J. Reilly, F. Reidinger, L.M. Corliss, J.M. Hastings, J. Less-Common Met. 88 (1982) 107.
[7] J.R. Johnson, J. Less-Common Met. 73 (1980) 345.
[8] J.R. Lacher, Proc. Roy. Soc. (London) 161A (1937) 525.
[9] W.L. Bragg, E.J. Williams, Proc. Roy. Soc. (London) 145A (1934) 699.
[10] J.R. Lacher, Proc. Cambridge Phil. Soc. 33 (1937) 518.
[11] M.H. Mintz, Z. Hadari, M. Bixon, Application of the Quasi-Chemical Approximation to Metal–Hydrogen Systems with One Type of Hydrogen Sites, Israel Atomic Energy Rep. NRCN-374, August 1974.
[12] M.H. Mintz, Thermodynamics and Statistical Mechanics of Some Hydrides of the Lanthanides and Actinides, Israel Atomic Energy Rep. NRCN-398, June 1976.
[13] O. Beeri, G. Kimmel, in: Advances in X-ray Analysis 41 (1998) by ICDD (on CD-ROM).
[14] Y. Osumi et al., J. Less-Common Met. 89 (1983) 257.
[15] K. Hiebl, Mat. Res. Bull. 17 (1982) 757.
[16] C.E. Lundin et al., Fourth Interim Progress Report — Development of Hydrogen Storage Materials for Application to Energy Needs, October 1978.